Investigation on Thermoacoustic Cooling Device with Variation in Stack Plate Size and Input Acoustic Energy

Nandy Putra and Dinni Agustina

Abstract A loudspeaker-driven thermoacoustic cooler device has been designed, constructed and tested to gain better understanding of its cooling performance. The influence of stack plate size to its performance was investigated. The plate was made of acrylic sheet in three different length variations, which were 6, 5 and 4. Each variation of experiment was conducted by varying plate thickness of the stack, 0.15, 0.5 and 1 mm, respectively. The experiments were conducted with various driver voltage input starting from setting 4–9 (Voltage peak-to-peak). The temperatures at the area of both ends of the parallel plate stack, which are cold side and hot side, were recorded. The results showed that thermoacoustic cooling effect occurred immediately and escalated rapidly in 2 min and showed a stable cooling temperature after 10 min. The experimental results confirmed that better thermal performance of the device and faster cooling rate yielded from higher voltage input. For each set of experiment, the input voltage setting, the operating frequency and other parameter of the stack were maintained the same. The thermal performance and cooling rate increased with the decrease of plate thickness. The largest temperature difference, 14.7 °C, was achieved with 0.15 mm plate thickness with 6 cm length at voltage setting 9. The experimental results showed that the effects of using different plate length were not the same for each thickness of stack plate. However, Stack plate size of 0.5 mm thickness and 6 cm length at the input voltage setting of 9, was arguably the optimum size in terms of consistent performance in cooling.

N. Putra (✉)
Applied Heat Transfer Laboratory, Department of Mechanical Engineering,
University of Indonesia, Kampus UI, Depok 16426, Indonesia
e-mail: nandyputra@eng.ui.ac.id

D. Agustina
Department of Mechanical Engineering, Syiah Kuala University, Darussalam,
Banda Aceh, Indonesia

1 Introduction

Refrigeration has been playing important role in almost every aspect of life to the level that living without it is impossible. It is even rated by the National Academy of Engineering as the 10th position in "Greatest engineering achievement in the 20th century" [1]. Despite the advantages, refrigeration's high demand of energy and the use of harmful refrigerants have been some of major concerns in the obligatory need of greener technologies in the future. Therefore, the focus of efforts is not only the engineering aspects of aimed at improving engine efficiency but also reducing the use of fossil fuels and chlorofluorocarbons/hydrochlorofluorocarbons (HFCs/HCFCs) as refrigerant. The hazard rate of HFC/HCFC to the atmospheric layer is about 2,000–3,000 times greater than carbon dioxide [2].

To answer the challenges of the environmental impact of the use of conventional refrigerants, one alternative developed is thermoacoustic technology devices which convert heat energy to sound energy and vice versa. The former is known as thermoacoustic engines or prime movers and the latter is called thermoacoustic heat pumps or refrigerators. This alternative is an environmentally friendly because it uses harmless working gas. In addition, this machine can operate with relatively low maintenance costs are because of the lack of moving parts and can take advantage of high amplitude sound waves and gas waste heat as the driving force [3]. The two main reasons above make thermoacoustic cooling technology more compelling to investigate.

Since 1980s, various designs of thermoacoustic heat engines have been built and tested in order to increase their performance and reliability [4] and large thermoacoustic heat engines was introduced in 1992 [5]. The same endeavour on development of heat pumps (refrigerators) has also made a launch since 1986 [6]. In 1993, the first spacecraft thermoacoustic cryocooler was developed and used in the space shuttle [7] and a breaking through temperature of −65 °C at cold side of a loudspeaker-driven thermoacoustic refrigerator was achieved in 2002 [8] by applying Rott's theories [9] and the modification of the theory by Hoffler and Swift [3, 10]. Noted that, these devices above are attractive for safer operation using air or inert gas and simplified manufacturing with much less moving parts in the system [11].

Since then, a great number of attention in the existing literature that worked in an attempt to build and increase the performance of the refrigerator. Three main aspects to concern in designing a thermoacoustic refrigerator are included but not limited to the operating condition, working fluid and the geometry of the refrigerator parts [12]. Higher performance and efficiency were aimed by experimentally lowering the Prandtl number of the working fluid [13]. Numerical efforts were also developed by increasing the ratio of acoustic pressure to mean pressure (drive ratio) [14] and simulating the effects of blockage ratio, the ratio of plate thickness and plate spacing [15]. Building an empirical equation for resonance frequency of the device which often shifts from its theoretical number was also attempted [16].

The heart of a thermoacoustic refrigerator acted as a compressor in a conventional refrigerator is called a stack. The dimension of the stack plays an important role due to heat transfer occurs around it have great impact on the thermal performance of the device. Amplitude of sound wave input (in terms of acoustic energy) and drive ratio will determine the cooling capacity and the efficiency that can be achieved. Therefore, these three will be one of the first things to approach in constructing a thermoacoustic refrigerator.

So far, the application of thermoacoustic principles can be used for heat engine (or power plant), heat pumps (or refrigerator) or a combination of both. Some examples of applications that have been and are being developed are as follows:

a. Liquefaction of natural gas. Acoustic energy to be used to pump heat to liquefy natural gas [17].
b. Chip cooling. Piezo-electric element produces sound waves. A heat pump cools the chip termoakustik work [18].
c. Electronics cooling on the ship. Loudspeakers produce sound waves and heat pump cools termoakustik electronic devices [7].
d. Electricity from concentrated solar energy generating acoustic waves in a heated termoakustik devices. A linear motor generates electricity from these products [19].
e. Cogeneration. Thermoacoustic heat engines generate acoustic energy from waste heat and linear motors convert acoustical energy into electricity.

2 Keypoints in Constructing the Thermoacoustic Refrigerator

The schematic presentation of λ/4 wavelength thermoacoustic refrigerator is shown in Fig. 1. It operates by using high amplitude sound waves and inert gases to produce cooling. The frequency of the driver, such as loudspeaker, and the
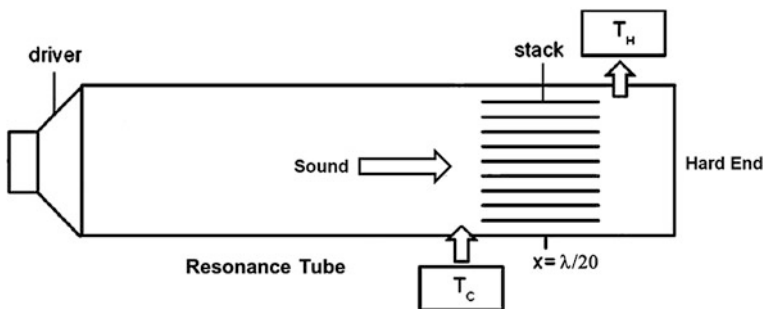

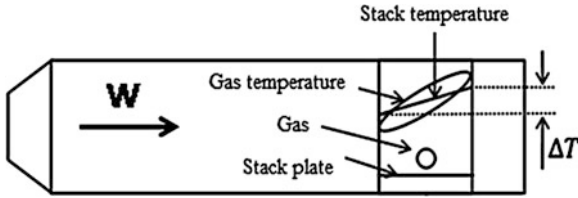**Fig. 1** The schematic of λ/4 wavelength thermoacoustic refrigerator

Fig. 2 The theoretical variations of stack and gas temperatures, and the temperatures at different locations inside and outside the stack, modified [20]

geometry of the resonator are calculated so as to get a standing sound wave in the resonator. A porous component called a stack is placed in the tube in such a way that a temperature difference due to thermoacoustic effect is created along the stack. One end of the stack starts to heat up while other end starts to cool down. By controlling temperature of hot side of stack (by means of a heat exchanger), the cold end of stack can provide lower temperature. There are five main components in a thermoacoustic refrigerator which are a resonator, a stack, a driver, working fluid and heat exchangers.

When there is no heat exchanger attached to the device, the fundamental study will be simplified. Such device is called thermoacoustic couples [4]. The theoretical variations of stack and gas temperatures is shown qualitatively in Fig. 2. ΔT is the difference in temperature of cold end and hot end of the stack. Acoustic power, W, is given by the speaker (driver) in the form of high amplitude sound waves. The length of the stack is assumed to be much less than the wavelength of the acoustic wave.

Main parts of the thermoacoustic couple including a sound generating device, resonance tubes, and stack. Besides greatly depending on the number of gas particles involved in the process, the system performance is also influenced by four main operational parameters (the drive ratio to excite thermoacoustic, operating frequency/resonance), the working fluid (Prandtl number), the geometry (blockage ratio, the diameter of the resonator, length of stack, stack position) and the material of stack and resonator [12].

2.1 Relation of the Resonance Frequency and Resonator

The design of the resonator tube having a major role to improve the efficiency of the thermoacoustic cooling device. Initial parameters are calculated based on the length of the resonator wavelength, λ. The length of resonator can be calculated by $\lambda/2$ or $\lambda/4$. The easiest way to decrease the acoustic power losses is to decrease the surface area of resonator wall; therefore the $\lambda/4$ wavelength resonator was chosen [3]. Theoretically, the resonator length, L = $\lambda/4$, giving ease of handling and dissipate only half the energy compared to the tube $\lambda/2$. Figure 3 shows some geometry of a resonator and resonator sections.
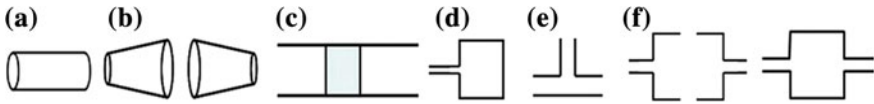
Fig. 3 Geometry of various resonators [21] **a** cylindrical or rectangular tube; **b** tapered tube; **c** capillary or tubule (regenerator); **d** Helmholtz resonator; **e** side tube; **f** reducer pipe

A smooth, linear cylindrical resonator without steps, misalignments and abrupt transition should be used to avoid unwanted eddying or non-linear pressure variations that would greatly complicated the analysis [17]. The length and diameter of resonator are 40 and 5.3 cm, respectively. The resonance frequency of sound wave is mainly determined by the length and the diameter of resonator [22].

$$f_n = \frac{nv}{4\left(L + \frac{14D}{23\pi}\right)}.$$ (1)

However, these theories must meet the result of the frequency test of the thermoacoustic device which was performed by inserting a condenser microphone into the resonator and connected it to the oscilloscope to get a relation between the frequency and its connecting voltage. The one with the highest voltage result was the resonance frequency which is best operating frequency for the device.

The material of resonator should be low in thermal conductivity and must endure vibration and pressure to the certain level. Acrylic tube was chosen because of these characteristics and its transparency help in order to arrange the stack and thermocouples and visualize them as well inside the resonator.

2.2 Driver

Thermoacoustic system is a thermodynamic cycle that is theoretically reversible. So that the driver of the heat pump can be either mechanical gas displacement system (such as speakers) or a heat engine. Loudspeakers are relatively easy to apply while the heat engine has a higher efficiency and has no moving parts [15].

2.3 Stack

The dimension of the stack should be around 10 % of the resonator volume and the spacing between the plates is determined by the thermal penetration depth of the stack which is 2–4 times the value of it [8]. In this experiment, acrylic sheet was cut into three different length which are 4, 5 and 6 cm with the wide adjusted to the inside diameter of the resonator. When the distance between the gas and the wall of

the stack is much larger than the thermal penetration depth, there will be an adiabatic heat transfer between the gas and the stack wall. Proposed optimum width is 2–4δk [4]. 4δk spacing was due to ease of fabrication [3], the distance 3δk obtained from experimental results [8] while the distance 2.2δk based on theoretical calculations and numerical [23]. The space between two plates ($2y_o$) is 0.55 mm (3δk).

$$\delta_k = \sqrt{\frac{k}{\pi \rho f c_p}}.$$
(2)

Low thermal conductivity and relatively large heat capacity is among the characteristics of the stack material to minimize heat transfer along the x-axis and maximize heat storing while phasing the sound wave in order to produce cooling effect [13]. Widely available acrylic sheet was chosen to meet these criterions. The variations of stack plate thickness ($2l_o$) are 0.15, 0.5 and 1 mm.

Besides δk, stack performance is also determined by its location in the resonator. Stack must be close to the antinode pressure to obtain a higher temperature variation in each packet due to higher gas pressure amplitude in the region towards the pressure antinode [24]. The stack was located at the distance of λ/20 from the closed end of the resonator [8] as this position will bring the optimum performance to the device because a well-balanced of pressure and velocity of the sound wave is achieved [5].

Figure 4a shows a cross sectional view of parallel plate stack, the blockage ratio is defined as the ratio of area available to gas in the stack to the total area of the stack. It is expressed as

$$BR = \frac{2y_0}{2y_0 + 2l_0}.$$
(3)

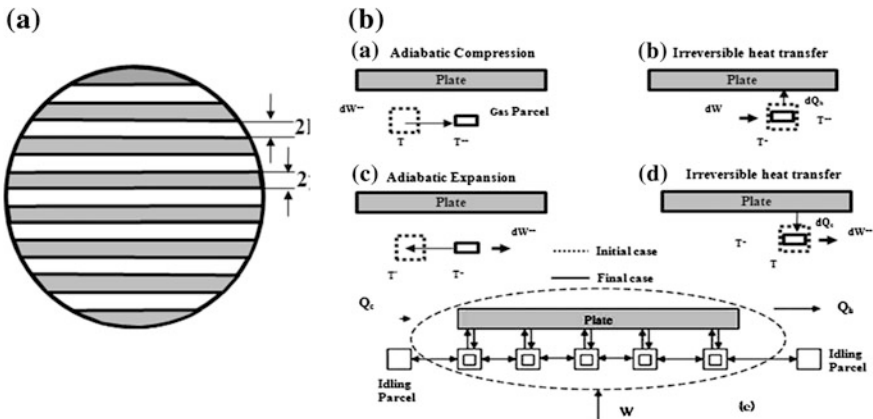
Fig. 4 **a** A cross sectional view of the stack. **b** Heat transfer between plate and gas parcels [25]

Figure 4b illustrates the gas parcels around the stack which experience displacement and temperature oscillation in association with the pressure variations with discrete steps as follows:

- When the gas is compressed, the temperature and the pressure will rise to T++ and P++, the heat will move from gas to the stack.
- After the heat transfer, the gas temperature and pressure will drop to T+ and pressure will remain P++. Gas will be expanded and moved back to its initial position with decreasing temperature.
- Gas temperature and pressure back to their initial value of T− and P. Stack temperature is higher than the temperature of the gas.
- Heat moves from the stack to the gas so that the gas pressure and temperature back to the initial state.

This phenomena which is induced by sound energy continues and generates temperature difference along the stack. Occurrence of the temperature difference will gradually end if the critical temperature gradient (∇T_{crit}) across the stack is equal to the local temperature gradient [17], where

$$\nabla T_{crit} = \frac{p}{\xi \rho c_p}. \tag{4}$$

p is the acoustic pressure and ξ is the acoustic displacement amplitude. This temperature is important in determining the properties of a thermoacoustic device, since efficiency depends on a temperature differential caused by the sound waves that is larger than the critical temperature so that a large cooling effect is created [8].

2.4 Drive Ratio

Variation of the drive ratio was done by adjusting the input voltage to the loudspeaker. Voltage variations made to vary the amplitude of the sound wave which is the refrigerator's driver. The greater the input voltage, the higher the pressure (amplitude) of sound waves. Peak-to-peak voltage were varied ranging from 1 to 9 Vpp on the function generator. Confirmation of waveforms, Vpp value and the RMS value of the input voltage is done by connecting a microphone on the end of the resonator to an oscilloscope.

2.5 Working Gas

The thermal penetration depth in designing stack also put into consideration the properties of working gas, which in this experiment was air. Air was chosen mainly because of its availability and its Prandtl number falls into the acceptable category of working gas for thermoacoustic device [13].

3 Procedure of the Experiments

Components of the refrigerator was fabricated or chosen based on the literatures. The resonator was built from a 40 cm straight acrylic tube. The internal diameter of the tube is 5.3 and the wall thickness is 3 mm. The length of the resonator was set equal to quarter of wavelength of the acoustic wave based on (2). Air at atmospheric pressure was used as a working fluid, as mentioned in Sect. 2.

An 8 Ω loudspeaker with the maximum power of 30 W was used as acoustic driver and installed at one end of the resonator. Another end was closed tightly using the same material as the resonator. After determining the operating frequency experimentally, the square wave at frequency 180 Hz was set in built-in function generator of a National Instrument Elvis II and the sound wave was amplified.

The length and the thickness of each stack plate were 6 cm and 1 mm, respectively. The stack was made of acrylic sheet and cut manually to fit into a cylindrical stack holder. The spacing between the plates was realized by gluing 0.55 mm fishing line on to the surface of each plate. Then the plates were arranged and glued in a stack holder made of the same material as the plates. The stack holder was inserted into the resonator. The fabrication of the stack was done in the same procedures for other sets of experiments with plate thicknesses of 0.5 and 0.15 mm and plate lengths of 5 and 4 cm, respectively.

Five type K thermocouples with accuracy of 0.05 were used; one for ambient temperature and two of those were inserted at different position at each end area of the stack. The temperature data from all thermocouples were acquired simultaneously every second by using National Instrument data acquisition module 9211. Both thermocouples at hot side read the same temperature while those at the cold side showed difference in reading of 1–2 °C. The lowest reading was featured on the graphs.

3.1 Experimental Set-Up

Experimental procedures should meet several requirements to better ensure the accuracy of the data recorded. Before carrying out experiments on the thermal performance of the thermoacoustic cooling device, some things to consider such as the time of experiment, setting the ambient temperature, thermocouple placement as well as the suitability of the basic theory is applied in the experimental set-up.

Besides the necessity of accurate data, precision is crucial in experiment so that any variation of the data should be repeated under the same conditions to record the data. Repetition also needs to be done in the opposite direction of variation.

Figure 5 shows the experimental setup of the thermoacoustic refrigerator constructed at the Heat Transfer Laboratory, University of Indonesia. The stack was placed at 6 cm from the closed end. The frequency and wave amplitudes were measured by a condenser microphone which was located at pressure anti node of
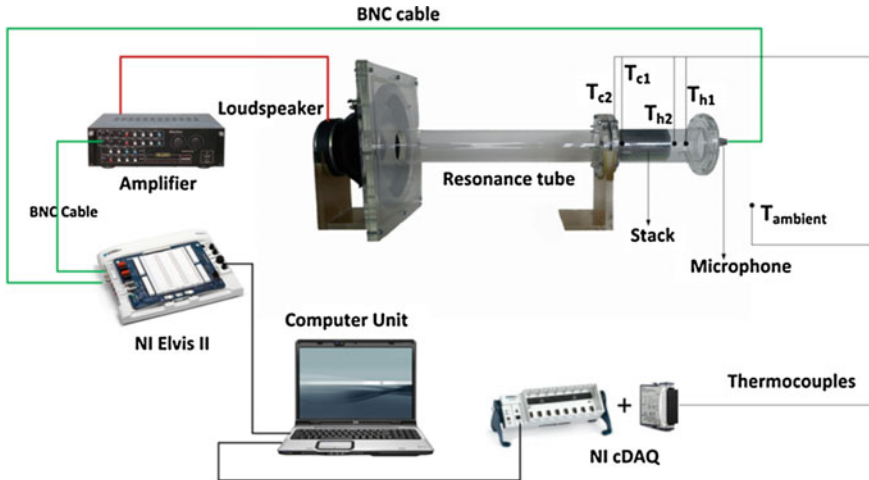
Fig. 5 The experimental set-up of the experiment

the resonator. The microphone was connected to a built-in oscilloscope of National Instrument Elvis II via Labview software. The oscilloscope confirmed the form and frequency of the wave input.

The experiment was conducted with variations in voltage peak to peak setting from 4 to 9 as the input voltage to the driver using a built in function generator in NI Elvis. The thickness of the plate stack was varied; 0.15, 0.5 and 1 mm. With each variation of the thickness, the length of the plate was also varied, 4, 5 and 6 cm. Figure 6 is the capture of one of the experiment that shows (a) the function generator used to input the sound wave and input voltage to the driver and (b) the oscilloscope monitor.
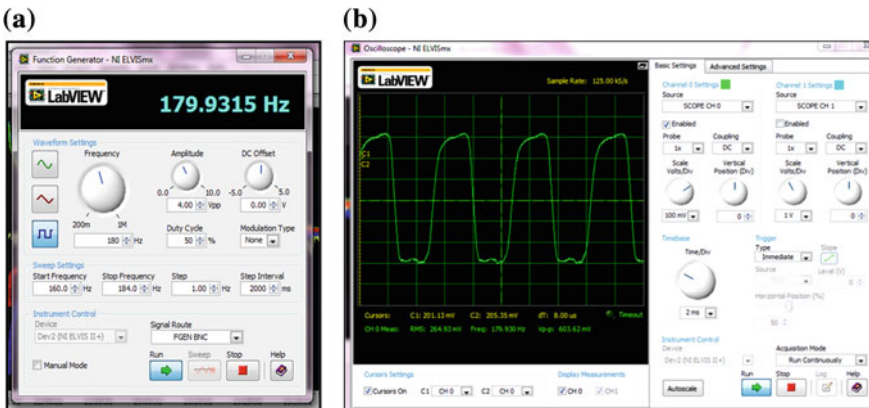

Fig. 6 Wave and voltage setting using national instrument Elvis II function generator (**a**) and **b** waveform and wave amplitude reading using NI Elvis II Oscilloscope

4 Result and Discussion

The theoretical resonance frequency for the resonator based on (2) is 209.6 Hz. The resonance frequency became around 180 Hz after installing the loudspeaker and placing the stack in the resonator. The existence of other structures and extra volume after the driver alter the resonance frequency [16]. 180 Hz is an approximation since the local temperature gradients established by the device alter the resonance frequency of the internal fluid [15].

Figure 7 shows the tested frequencies and their connecting voltage result at different positions; positions 1–6 which are near the edge of the tube, $\lambda/20$ from the driver, $\lambda/8$, at the middle of tube length, $\lambda/20$ from the tube end and the last one is the left end. The frequency that resulted higher voltage was considered as the resonance frequency which was consistently around 180 Hz.

Types of sound waves which are used as the input affect the temperature difference between both ends of the stack, as shown in Fig. 8. Both ends of the stack temperature difference is of 7.8 and 5 ° C respectively for the input square wave and sinusoidal wave input. Cooling is obtained by using a square wave remains stable up to 20 min, while cooling using sinusoidal wave decreases at about 10 min. Square wave has a higher energy than sinusoidal waves due to the strengthening of the amplitude.

4.1 Effect of Input Voltage Setting on Thermal Performance

To understand how sound wave amplitude affects the thermal performance of the resonator, sound wave amplitude was varied by setting the voltage peak to peak input from 4 to 9 with one increment for each experiment. The experiments were conducted for three different length of plate of 4, 5 and 6 cm, respectively. Figure 9

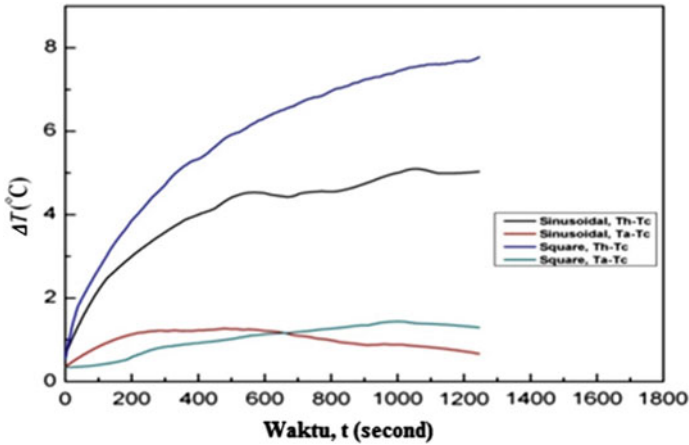**Fig. 7** Frequencies and their connecting voltage output at different position in resonator
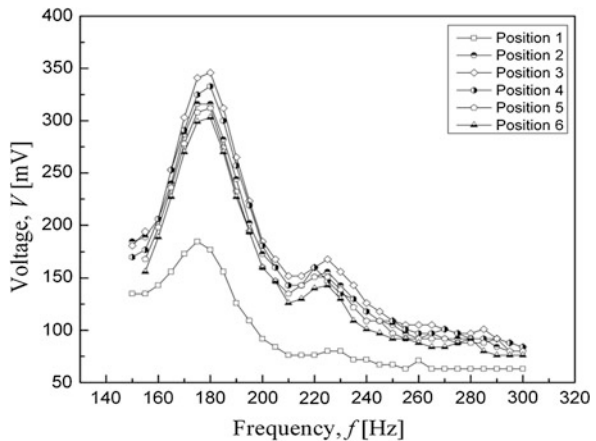
Fig. 8 Differences in temperature with different input wave

shows the performance for three variations on the thickness and the length of stack plate. Illustration of changes in ambient temperature difference and the cool side, the ambient temperature difference and the hot side and the cold side of the total temperature difference and heat each side indicated by $T_a - T_c$, $T_h - T_a$ and T_{total}. One block consists of four sections which represent data at 5, 10, 15 and 20 min duration.

The results showed that the length of 6 cm imply the largest temperature difference between cold and hot end of stack as shown in Fig. 9a–c. It is seen that the thermoacoustic phenomena inside the resonance tube yielded temperature difference between two extremities of the parallel plate stack. The result shown is the largest temperature difference, 14.8 °C achieved in 10 min time that occurred by using 0.15 mm plate thickness at input setting 9 Vpp.

Figure 10 presents the temperature difference across the stack yielded with various input voltage using 0.15 mm plate thickness. As expected the plot shows that higher input voltage will produce linearly higher temperature difference. The difference grows rapidly more than 50 % in 30 s and continues to around 80 % in 4 min and becomes generally constant in 10 min. These trends are in agreement to those shown in literature [26]. It is observed that starting from 10 min duration of experiment the local temperature gradient is relatively equal to the critical temperature gradient so that the acoustic energy have been fully used to overcome the heat dissipation [27].

The difference in temperature of the stack cold side (plate thickness of 0.15 mm) and the ambient temperature was plotted against time in Fig. 11. The data was recorded for 20 min with various input voltage to the loudspeaker. The figure shows that at 9 Vpp input to the driver the temperature of cold side decreased the most, 8.4 °C, in 90 s. The trend in Fig. 6 is similar to that found in the literature [28].
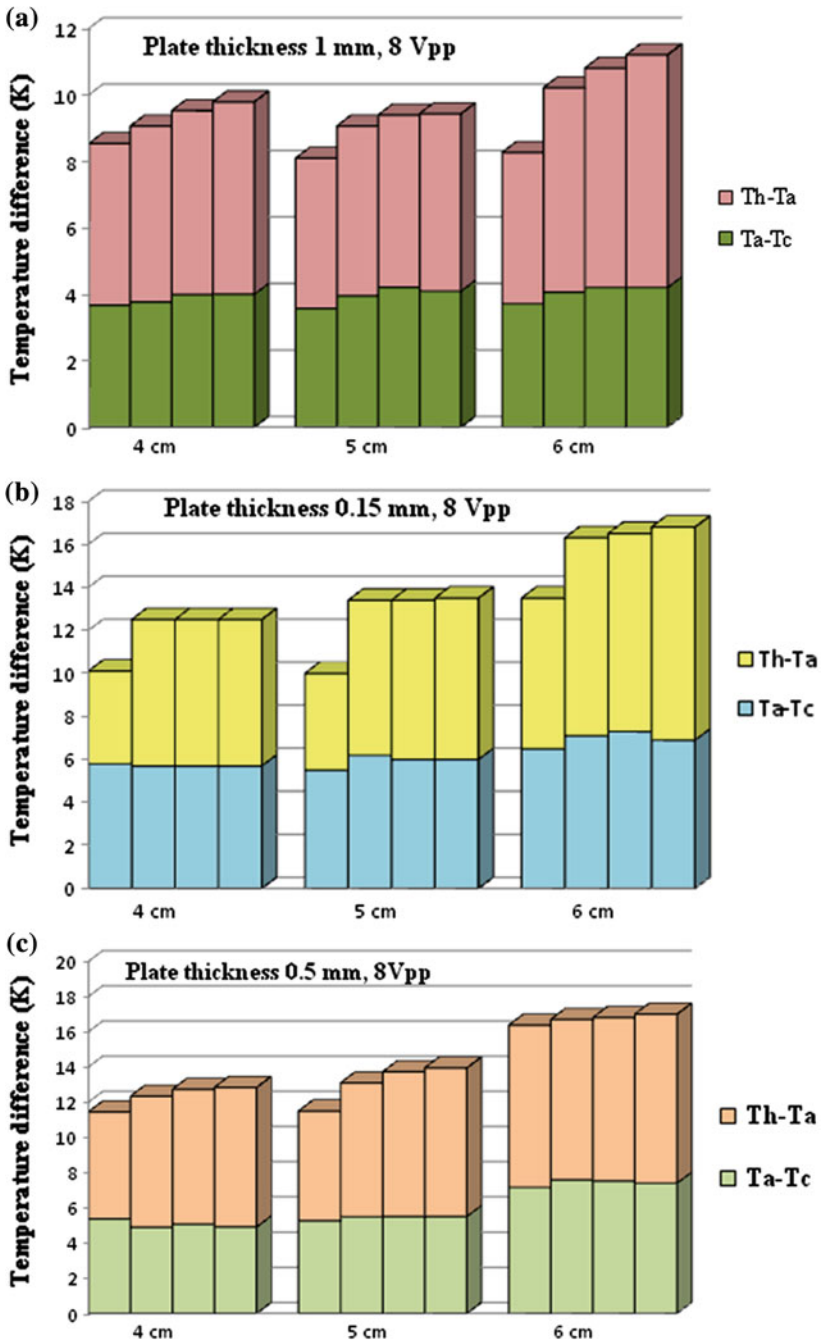
Fig. 9 Comparison of the results of the stack length 4–6 cm for **a** 1 mm thickness, **b** 0.15 mm thickness and **c** 0.5 mm thickness, on the temperature difference
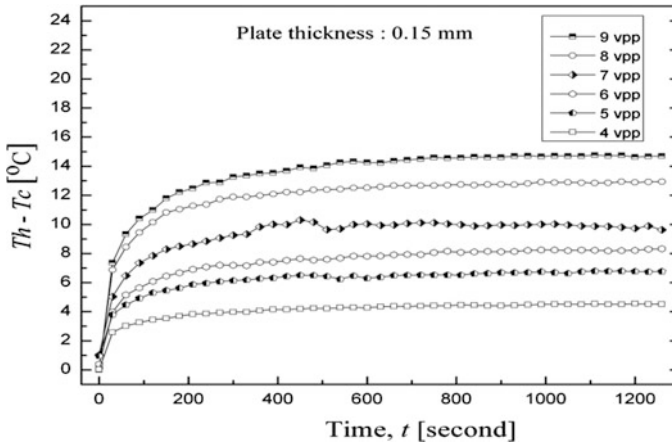
Fig. 10 The thermal performance of the resonator from 4 to 9 Vpp

The temperature then began fluctuating on the cold side of the stack due to drifting of thermocouples but it stayed lower than others. The figure also indicates that the cooling rate with input voltage 8 and 9 were faster than other input voltages although the trends are similar for all variations. The data was also recorded for different plate thickness, 0.5 and 1 mm with various input voltage. All measurements were recorded in a room with 26.5 °C ambient temperature (T_a).

4.2 The Effect of Plate Thickness on the Thermal Performance and Cooling Rate

Figure 9 depicts that using stack plate of 0.15 mm thickness produced the largest temperature difference across the stack and the fastest cooling rate compared to plate thickness of 0.5 and 1 mm. The input voltage to the driver remained constant during the experiment. At 9 Vpp, the largest temperature difference ($T_h − T_c$) for plate thicknesses of 0.15, 0.5 and 1 mm were 14.8, 13.1 and 9.2 °C respectively. It indicates that for the given resonator geometry, thinner plates means lower blockage ratio and produces higher thermal performance as found in literature [29].

Figure 9 also shows that at the same condition of input voltage, decrease in temperature at cold side of the stack ($T_c − T_a$) were up to 8.1, 7 and 4 °C for plate thicknesses of 0.15, 0.5 and 1 mm, respectively. It was observed from the experiment that thinner stack plate shows faster cooling rate at the cost more effort in fabricating the stack plate and deterioration of the stack plate after several set of experiment due to less rigidity in material used for the stack, as shown in Fig. 12.
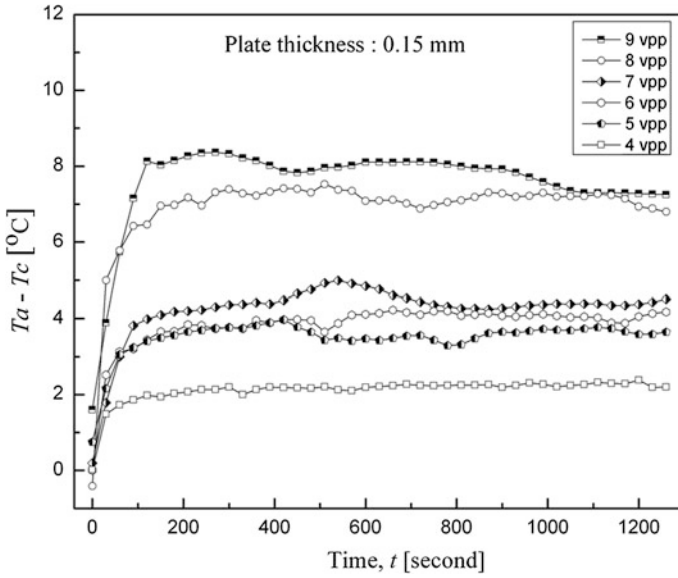
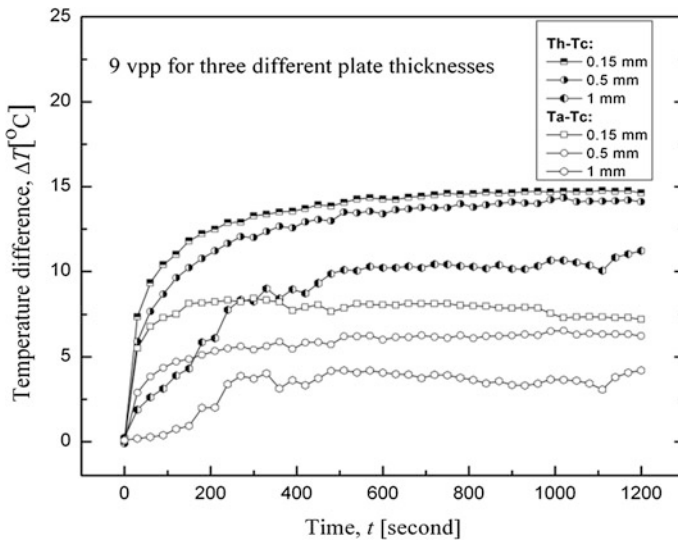**Fig. 11** Cooling rate of cold side of the stack, plate thickness of 0.15 mm

Fig. 12 Thermal performance and cooling rate with variation in stack plate thickness at 9 Vpp

5 Conclusions

The performance of the refrigerator in terms of temperature difference produced at the ends of the stack and the cooling rate were observed. The results showed that higher amplitude of sound wave (ranging from 4 to 9 Vpp setting) produce larger temperature difference, as expected. The experimental result showed that using plate with thickness of 0.15 mm and length of 6 cm at 9 Vpp yielded the largest temperature difference when compared to 0.5 and 1 mm plate for the given length and input voltage to the driver. Decrease in plate thickness leads to significant increase in cooling rate; which are for 0.15 mm plate thickness temperature dropped 8.5 °C below the ambient temperature in 2 min. For 0.5 and 1 mm plate thicknesses, the temperature drops 5 and 1 °C, respectively, below ambient in the same amount of time. Thinner plates which provide more area for heat transfer relative to the given resonator ensure faster cooling rate. However, whether the thinnest is the most optimum one still needs further study since by using plate of 0.5 mm thickness the cooling effect was more consistent and the stack structure was much more rigid compared to others.

References

1. Poesse ME (2012) Handbook of climate change mitigation. Springer, New York, pp 1821–1848
2. Lackner M, Chen W-Y, Suzuki T (2012) Introduction to climate change mitigation. Handbook of climate change mitigation. Springer, New York, pp 1–14
3. Swift G (2001) Thermoacoustics: a unifying perspective for some engines and refrigerators. J Acoust Soc Am 113(5):2379–2381
4. Wheatley J, Hofler T, Swift GW, Migliori A (1985) Understanding some simple phenomena in termoakustiks with applications to acoustical heat engines. Am J Phys 53:147–162
5. Swift GW (1992) Analysis and performance of a large thermoacoustic engine. J Acoust Soc Am 92:1551–1563
6. Hofler TJ (1986) Thermoacoustic refrigerator design and performance. PhD thesis, Physics Department, University of California, San Diego
7. Garret SI, Adeff JA, Hofler TJ (1993) Thermoacoustic refrigerator for space application. J Thermophys Heat Transf 7:595–599
8. Tijani MEH, Zeegers JCH, De Waele ATAM (2002) Construction and performance of a thermoacoustic refrigerator. Cryogenics 42(4):59–65
9. Rott N (1980) Thermoacoustics. J Adv Appl Mech 20:135–175
10. Swift GW (1988) Thermoacoustic engines. J Acoust Soc Am 84(4):1145–1180
11. Zink F, Vipperman J, Schaefer L (2010) CFD simulation of thermoacoustic cooling. Int J Heat Mass Transf 53:3940–3946
12. Ghorbanian K, Hosseini H, Jafargholi M (2008) Design road-map for thermoacoustic refrigerators. J Acoust Soc Am 123(5):3546
13. Tijani MEH, Zeegers JCH, De Waele ATAM (2001) Prandtl number and thermoacoustic refrigerator. J Acoust Soc Am 112(1):134–143
14. Tasnim SH, Mahmud S, Fraser RA (2012) Effect of variation in working fluids and operating conditions on the performance of a thermoacoustic refrigerator. Int Commun Heat Mass Transf 39:762–768

15. Zoontjens L (2008) Numerical investigations of the performance and effectiveness of thermoacoustic couples. Ph.D Dissertation, School of Mechanical Engineering, University of Adelaide. http://digital.library.adelaide.edu.au/
16. Ghazali NM, Ghazali AD, Ali IS, Rahman MAA (2012) Geometry effects on cooling in a standing wave cylindrical thermoacoustic resonator AIP Conf Proc 1440:1320
17. Wollan JJ, Swift GW, Backhauss SN, dan Gardner DL (2002) Development of a thermoacoustic natural gas liquefier. In: Proceedings of AICHE meeting, New Orleans
18. Symco O, Abdel Rahman E, Kwon Y, Behunin R (2004) Design and development of high-frequency thermoacoustic engines for thermal management in microelectronics. Microelectron J 35:185
19. Adeff JA, Hofler TJ (2000) Design and construction of a solar powered, thermoacoustically driven thermoacoustic refrigerator. J Acoust Soc Am 107(6):37–42
20. Babaei H, Siddiqui K (2011) Modified theoretical model for thermoacoustic couples. Int J Therm Sci 50:206–213
21. Qing E, Feng W, Duan Yong L (2009) Thermoacoustic refrigeration device. http://ieeexplore.ieee.org/iel5/4918025/4918026/04918931
22. Moloney MJ, Hatten DL (2001) Acoustic quality factor and energy losses in cylindrical pipes. Am J Phys 69(3):311–314
23. Arnott WP, Bass HE, Raspet R (1991) General formulation of thermoacoustic for stack having arbitrarily shaped pore cross sections. J Acoust Soc Am 90:3228–3237
24. Wetzel M, dan Herman C (1997) Design optimization of thermoacoustics refrigerators. Int J Refrig 20:3–21
25. Ghazali NM, Aziz AA, Rajoo S (2006) Environmentally friendly refrigeration with Thermoacustic research vote: 74166. University of Technology, Malaysia
26. Hariharan NM, Sivashanmugam P, Kasthurirengan S (2012) Influence of stack geometry and resonator length on the performance of thermoacoustic engine. Appl Acoust 73:1052–1058
27. Xiao JH (1995) Thermoacoustic heat transportation and energy transformation. Part 3: adiabatic wall thermoacoustic effect. Cryogenics 35:27
28. Russell DA, Weibull P (2002) Tabletop thermoacoustic refrigerator for demonstrations. Am J Phys 70(12)
29. Akhavanbazaz M, Siddiqui MHK, Bhat RB (2007) The impact of gas blockage on the performance of a thermoacoustic refrigerator. Exp Thermal Fluid Sci 32:231–239